

Raman G and D band in strongly photoexcited carbon nanotubes

Pascal Puech,^{1,*} Abdul Waheed Anwar,¹ Emmanuel Flahaut,² David J. Dunstan,³ Ayman Bassil,⁴ and Wolfgang Bacsa¹

¹*CEMES, CNRS, Université de Toulouse, 29 rue Jeanne Marvig, 31055 Toulouse, France*

²*CIRIMAT, CNRS/UPS/INPT, LCMIE Bat. 2R1, 118 Route de Narbonne 31062, Toulouse cedex 9, France*

³*Department of Physics, University of London, Queen Mary, London E1 4NS, United Kingdom*

⁴*Faculté des Sciences II, Université Libanaise, BP 90656 Fanar, Lebanon*

We observe clear differences in the spectral shift of the Raman D and G bands when heating double wall carbon nanotubes through intense photon irradiation and by varying the temperature in a thermostat. These spectral differences are attributed to modifications of the defect induced double-resonance Raman process, and are consistent with Stokes–anti-Stokes anomalies observed for single and double wall carbon nanotubes, not present in graphite. We find that the Raman intensity for double wall carbon nanotubes increases superlinearly in the red spectral region and sublinearly in the UV spectral region.

DOI: [10.1103/PhysRevB.79.085418](https://doi.org/10.1103/PhysRevB.79.085418)

PACS number(s): 61.46.Np, 63.20.kd, 65.40.–b

I. INTRODUCTION

Carbon nanotubes (CNTs) are widely studied for their potential use in optoelectronic devices, high-density memory, and nanostructured materials.¹ Resonant excitation of CNTs makes optical techniques highly sensitive. Raman spectroscopy is an ideal tool in screening tubes through spectral mapping² to detect defects caused by the appearance of the D band and to determine the tube diameter through the radial breathing mode (RBM).³ The influence of the formation of excitons associated to strong electron-phonon coupling on the observed spectra has only been explored recently.^{4–8} In single wall carbon nanotubes (SWs), the G band is split into two bands (G_- , G_+). The G_- band has first been attributed to the zone-center optical mode in circumferential direction. Later *ab initio* calculations, including electron-phonon coupling, have shown that this assignment depends on whether the tube is semiconducting or metallic.⁶ For isolated metallic tubes the LO mode is expected to be strongly downshifted corresponding to G_- while the TO mode remains less intense due to absorption when the electric field is oriented along the tube axis. For semiconducting tubes, G_+ corresponds to the LO mode and has a higher intensity than the G_- band. For double wall carbon nanotubes (DWs), the inner tube is coupled to the outer tube and the two walls give rise to a single G band with two main components at 1581 (inner tube) and 1592 cm^{-1} (outer tube).⁹ The RBMs of inner tubes in DWs are found to be dependent on the tube growth process.⁸ For multiwall carbon nanotubes (MW) a shoulder at the high energy side of the G band appears (D' : around 1620 cm^{-1}) which is not removed even after annealing.¹⁰ In this paper, we compare D and G band shifts as a function of laser power in air and by changing the temperature in a methanol heat bath. Differences in spectral shifts of the D and G bands are then compared with Stokes (S) and anti-Stokes (AS) spectra recorded in function of laser irradiation.

II. SAMPLES AND EXPERIMENTS

DWs have been prepared by the catalytical chemical vapor deposition method (CCVD) as described in Ref. 11.

High-resolution electron microscopy (Fig. 1) shows the presence of small bundles of DWs with diameters ranging from 0.6 to 3.0 nm.

Raman spectra have been recorded using Renishaw (633 nm), Dilor XY visible (647 nm), and Dilor XY UV (338 nm) spectrometers. We compare spectra recorded with two different spectrometers working in the visible spectral range to detect possible differences in the spectrometer characteristics which depends on grating and microscope used. One charge-coupled device (CCD) pixel corresponds to 1 cm^{-1} for the Renishaw and 0.7(2) cm^{-1} for the visible (UV) Dilor spectrometer. When mapping strained silicon we have obtained a spectral error smaller than 0.05 cm^{-1} when fitting the optical phonon band. All phonon bands have been fitted with a Lorentzian line shape.

III. TEMPERATURE INDUCED SHIFTS OF THE RAMAN D AND G BANDS

A. Changing the temperature using a thermostat

We have used methanol to thermalize DWs. Pieces of agglomerated DWs are immersed in methanol without sonication. The spectral D and G band positions are uniform

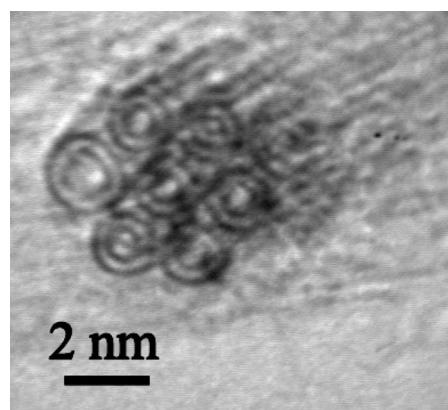


FIG. 1. Bundle of DWs observed by high-resolution transmission electron microscopy.

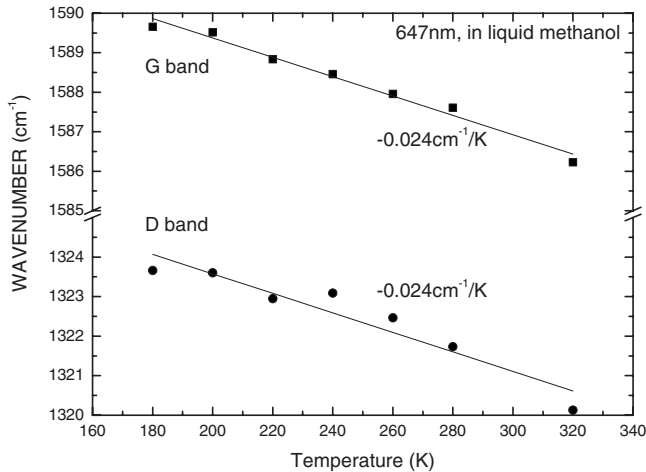


FIG. 2. *D* and *G* band positions of DWs in methanol as a function of temperature.

across different locations of the sample at low laser power ($1 \text{ mW}/\mu\text{m}^2$). We have varied the temperature from 180 to 320 K using a cryostat. Figure 2 shows the temperature dependence of the *D* and *G* band positions after fitting the recorded spectral bands.

We observed that the *D* and *G* bands shift to lower energies at the same rate with increasing temperature ($-0.024 \text{ cm}^{-1}/\text{K}$).^{12,13} For CNTs in methanol, however, the laser power which can be applied is limited. Optical absorption by the DWs increases the local temperature and the surrounding liquid. At the boiling point of methanol, vaporization takes place ($65 \text{ }^\circ\text{C}$) and the agglomerated DWs drift out of the focal point. The rate at which the *D* and *G* bands shift is consistent with what has been reported earlier. For suspended tubes a similar temperature coefficient ($-0.022 \text{ cm}^{-1}/\text{K}$) has been reported.¹⁴ Chiashi *et al.*¹⁵ has observed RBMs and *G* band from 100 to 1000 K, and found a similar temperature coefficient of the *G* band ($-0.031 \text{ cm}^{-1}/\text{K}$) in the linear range, i.e., temperature higher than 300 K.

B. Temperature change through photoexcitation

We have irradiated DWs in air with increasing laser power (633 nm, 1–100 mW). Photoabsorption leads to considerable heating of the DWs which depends strongly on wavelength of the incident beam¹² and is limited by the oxidation of the tubes. Excitation with a shorter wavelength leads to a large increase in temperature at constant laser power. At lower laser power (633 nm, 1–10 mW) the *G* band shifts by less than 1 cm^{-1} corresponding to temperatures close to room temperature (10 mW: 1588.8 cm^{-1} ; 1 mW: 1589.2 cm^{-1}). When increasing laser irradiation we find that the spectral shifts for the *G* and *D* bands are nonlinear and different for the two bands as reported in Fig. 3.

To understand the differences in the spectral shifts of the *D* and *G* bands when heating by photoabsorption or in a thermostat, we have recorded Stokes and anti-Stokes spectra. Anti-Stokes Raman spectra have been analyzed in detail for

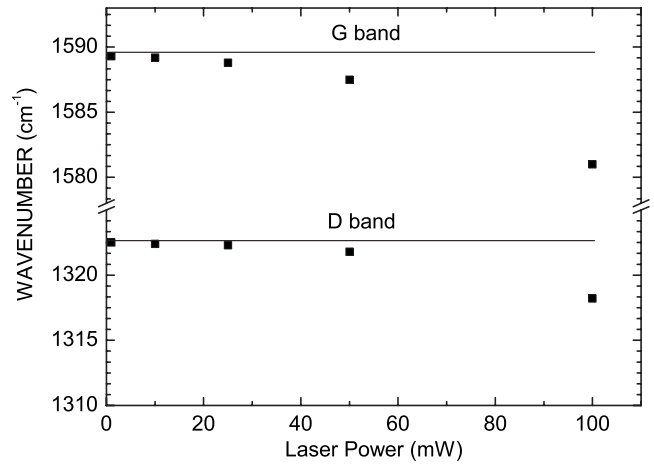


FIG. 3. DWs wave number versus the laser power (633 nm).

graphite, graphitic whiskers,¹⁶ MWs,¹⁷ and SWs.¹⁸ Due to the low intensity of the anti-Stokes spectrum at room temperature, it is challenging to obtain spectra far from the Rayleigh line.¹⁹ The anti-Stokes spectrum is reduced by a factor of 2000 when compared to the Stokes spectrum at room temperature considering the Bose-Einstein factor with $\omega = 1600 \text{ cm}^{-1}$. Figure 4 shows Stokes and anti-Stokes spectra recorded at 50 and 100 mW. The spectra recorded at 100 mW laser power have *D* and *G* bands shifted to lower energy when compared to the spectra recorded at 50 mW due to stronger laser heating. We find that the *G* band shift is nearly two times as large as the *D* band shift for both Stokes and anti-Stokes spectra for the two spectra. This shows that there is a fundamental difference when heating CNTs at high laser power. In order to compare the Stokes and anti-Stokes spectra, we assume that temperature induced shifts of the electronic levels is negligible in comparison to the width of electronic resonance profile for the *G* band. For temperature induced shifts of the electronic transitions, we expect $3 \text{ meV}/100 \text{ K}$ for the E_{11} transition²⁰ which is significantly smaller

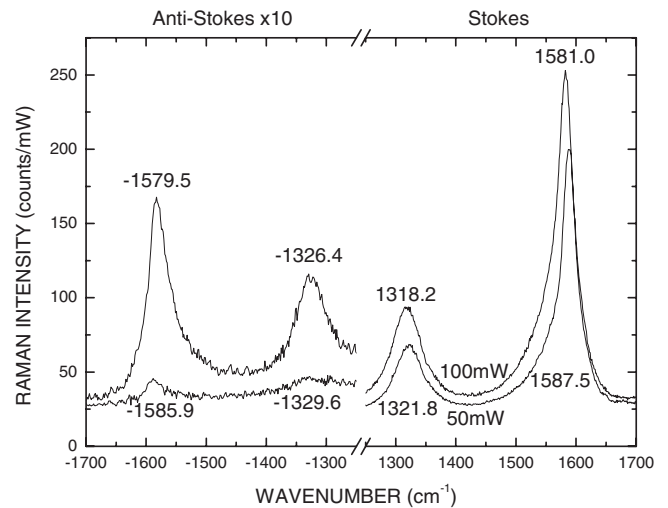


FIG. 4. Raman spectra of DWs recorded with 50 and 100 mW (633 nm). The spectra are scaled to the incident laser power. The anti-Stokes spectra have been multiplied by a factor of 10.

TABLE I. Parameters deduced from the S and AS spectra in Fig. 4

Values	<i>D</i> band	<i>G</i> band
$\frac{1}{T_{50 \text{ mW}}} - \frac{1}{T_{100 \text{ mW}}} (\text{S/AS})$	$-8.57 \times 10^{-4} \text{ K}^{-1}$	$-8.65 \times 10^{-4} \text{ K}^{-1}$
$\omega(T_{50 \text{ mW}}) - \omega(T_{1 \text{ mW}}) (\text{S})$	-0.8 cm^{-1}	-1.7 cm^{-1}
$\omega(T_{100 \text{ mW}}) - \omega(T_{1 \text{ mW}}) (\text{S})$	-4.4 cm^{-1}	-8.2 cm^{-1}

than the lower limit of the resonance profile for isolated suspended tubes of 80 meV.²¹ The anti-Stokes spectra of RBMs of SWs has been studied in detail by Brown *et al.*,²² demonstrating that the spectra on the Stokes and anti-Stokes sides correspond to tubes of different chirality or helicity due to the different resonant condition for Stokes and anti-Stokes spectra. For DWs, however, coupling of the walls and large size distribution broaden the *G* band resonance. To eliminate common factors in the spectra, we take the ratio of the Stokes and anti-Stokes spectra recorded at different laser irradiation:

$$\frac{\frac{I_S}{I_{AS}}(T_{100 \text{ mW}})}{\frac{I_S}{I_{AS}}(T_{50 \text{ mW}})} = \frac{e^{\hbar\omega/(k_B T_{100 \text{ mW}})}}{e^{\hbar\omega/(k_B T_{50 \text{ mW}})}} = e^{1.44\omega[(1/T_{100 \text{ mW}})-(1/T_{50 \text{ mW}})]},$$

where T is in K and ω in cm^{-1} .

By taking the ratio of the spectra we eliminate the ω^4 factor and the electronic contributions to the spectra. It is assumed that the temperature distribution is homogenous. We can deduce the difference of the inverse temperature using the two spectra recorded at two different laser powers, and compare these with the measured frequency shifts of the *D* and *G* bands (Table I). When taking the ratio of the integrated intensity of the *G* and *D* bands in deducing the difference of the inverse temperature, we find that the intensity variation in the *G* and *D* band are similar.

Table I shows that the *D* band shift is significantly smaller compared to the *G* band shift both at 50 and 100 mW. The inverse temperature for the *G* band deduced from the band shift is close to the value obtained from the ratio of the Stokes/anti-Stokes spectra while for the *D* band the corresponding value is 30% lower. This demonstrates that the *D* band position is influenced by laser irradiation. The ratio of the two spectra recorded at different laser power gives the opportunity to compare the differences in the *D* and *G* band positions attributed to differences in phonon temperature with the temperature deduced from the ratio of the Stokes and anti-Stokes spectra. Differences in phonon temperature due to nonequilibrium phonons would, however, imply changes in the relative *D* and *G* band intensities. Clearly laser irradiation leads to the creation of a larger number of excitons. The presence of excitons modifies the electronic and the local tube structures. When recording laser power dependent Raman spectra of different types of tubes (SW, MW, and doped MW), we find no uniform shift of the *D* and *G* bands; $\Delta\omega_D/\Delta\omega_G$ varies between zero to one. At 468 nm and for DWs, $\Delta\omega_G=12.5 \text{ cm}^{-1}$ while $\Delta\omega_D=6.0 \text{ cm}^{-1}$,

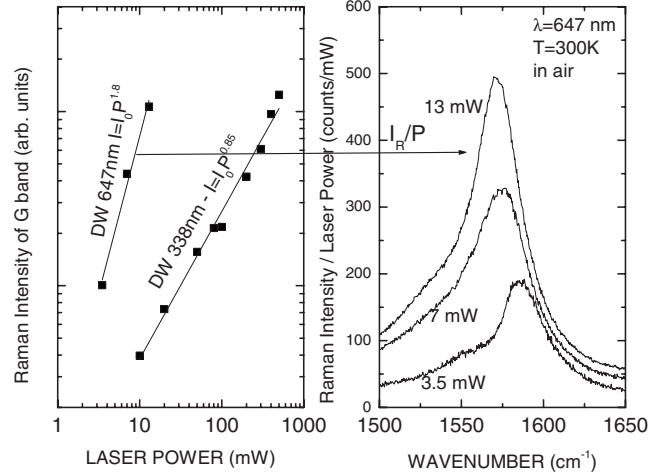


FIG. 5. Raman intensity as a function of laser power. Excitation wavelength of 647 nm.

for SWs $\Delta\omega_G=8.5 \text{ cm}^{-1}$ while $\Delta\omega_D=3.5 \text{ cm}^{-1}$, and for nitrogen-doped MWs, the *D* band remains unaffected while *G* band downshifts. With UV excitation, we find that the *G* and *D* bands are the same for SWs. While the *G* band shifts are consistent with the corresponding Stokes/anti-Stokes spectra, the *D* band shift is nonuniform at high laser irradiation. *D* band shifts are not only attributed to temperature variations but also appear to be connected to the presence of excitons. Apart from the nonlinear shifts of the *D* and *G* bands with laser irradiation, Fig. 4 shows that the intensity of the two bands is superlinear when increasing the laser irradiation.

IV. LASER POWER DEPENDENCE OF SPECTRAL INTENSITY

To explore the differences in the resonance conditions for different excitation wavelengths, we have compared the power scaled intensity of the *G* band. Figure 5 shows the variation in the integrated intensity of the *G* band as a function of laser power excited at 647 and 338 nm. We find that the normalized intensity as a function of laser power follows a power law. The Raman intensity is smaller when excited at 338 nm as compared when excited at 647 nm. The same is observed when using a different spectrometer (Renishaw at 633 nm) to exclude the influence of detector response and spectrometer performance. When excited at 647 nm, the integrated intensity increases superlinearly while when excited at 338 nm, the intensity increases sublinearly. Sublinear behavior can be explained by heat induced broadening of the electronic bands due to strong absorption in the UV spectral range which reduces the Raman cross section. Superlinear behavior can be explained by participation of excitons in the resonance process as observed in strained GaAs,^{23,24} or by exciton screening resulting in changes in the joined density of states.

V. CONCLUSION

We observe clear differences in the *D* and *G* band Raman shifts at high photon irradiation of carbon nanotubes. Com-

parison with the Stokes and anti-Stokes spectra show that the *D* band shift is reduced at high photon irradiation and depends on tube type. The changes in the *D* band shift are attributed to the modification of the electronic band structure through the creation of excitons. Superlinear and sublinear intensity increases in the phonon bands with laser power are observed when using excitation in the red and UV spectral range, respectively, and attributed to participation of excitons

in the double-resonance process and heat induced broadening of the electronic bands due to strong absorption.

ACKNOWLEDGMENTS

A. W. A. acknowledges the financial support of the Higher Education Commission of Pakistan.

*Pascal.Puech@cemes.fr

- ¹ *Understanding Carbon Nanotubes, from Basics to Application*, edited by A. Loiseau, P. Launois, P. Petit, S. Roche, and J. P. Salvetat (Springer, New York, 2006).
- ² 4th Intel Ireland Research Conference and Raman Workshop, 10–12 September 2007 (unpublished).
- ³ M. S. Dresselhaus, G. Dresselhaus, and P. Avouris, *Carbon Nanotubes: Synthesis, Structure, Properties and Applications*, 1st ed. (Springer, New York, 2001).
- ⁴ S. M. Bachilo, M. S. Strano, C. Kittrell, R. H. Hauge, R. E. Smalley, and R. B. Weisman, *Science* **298**, 2361 (2002).
- ⁵ C. D. Spataru, S. Ismail-Beigi, L. X. Benedict, and S. G. Louie, *Phys. Rev. Lett.* **92**, 077402 (2004).
- ⁶ S. Piscanec, M. Lazzeri, J. Robertson, A. C. Ferrari, and F. Mauri, *Phys. Rev. B* **75**, 035427 (2007).
- ⁷ M. Machon, S. Reich, and C. Thomsen, *Phys. Rev. B* **74**, 205423 (2006).
- ⁸ *Carbon Nanotubes*, Topics in Applied Physics, No. 111, edited by A. Jorio, M. S. Dresselhaus, and G. Dresselhaus (Springer, New York, 2008).
- ⁹ P. Puech, A. Ghandour, A. Sapelkin, C. Tinguely, E. Flahaut, D. J. Dunstan, and W. Bacsá, *Phys. Rev. B* **78**, 045413 (2008).
- ¹⁰ K. Behler, S. Osswald, H. Ye, S. Dimovski, and Y. Gogotsi, *J. Nanopart. Res.* **8**, 615 (2006).
- ¹¹ E. Flahaut, R. Bacsá, A. Peigney, and Ch. Laurent, *Chem. Commun. (Cambridge)* **12**, 1442 (2003).
- ¹² A. Bassil, P. Puech, L. Tubery, W. Bacsá, and E. Flahaut, *Appl. Phys. Lett.* **88**, 173113 (2006).
- ¹³ P. Puech, E. Flahaut, A. Bassil, T. Juffmann, F. Beuneu and W. S. Bacsá, *J. Raman Spectrosc.* **38**, 714 (2007).
- ¹⁴ I. K. Hsu, R. Kumar, A. Bushmaker, S. B. Cronin, M. T. Pettes, L. Shi, T. Brintlinger, M. S. Fuhrer, and J. Cumings, *Appl. Phys. Lett.* **92**, 063119 (2008).
- ¹⁵ S. Chiashi, Y. Murakami, Y. Miyauchi, and S. Maruyama, *Jpn. J. Appl. Phys.* **47**, 2010 (2008).
- ¹⁶ P. H. Tan, C. Y. Hu, J. Dong, W. C. Shen, and B. F. Zhang, *Phys. Rev. B* **64**, 214301 (2001).
- ¹⁷ P. H. Tan, L. An, L. Q. Liu, Z. X. Guo, R. Czerw, D. L. Carroll, P. M. Ajayan, N. Zhang, and H. L. Guo, *Phys. Rev. B* **66**, 245410 (2002).
- ¹⁸ J. Maultzsch, S. Reich, and C. Thomsen, *Phys. Rev. B* **70**, 155403 (2004).
- ¹⁹ P. Puech, E. Flahaut, A. Sapelkin, H. Hubel, D. J. Dunstan, G. Landa, and W. S. Bacsá, *Phys. Rev. B* **73**, 233408 (2006).
- ²⁰ D. Karaiskaj, C. Engtrakul, T. McDonald, M. J. Heben, and A. Mascarenhas, *Phys. Rev. Lett.* **96**, 106805 (2006).
- ²¹ C. Fantini, A. Jorio, M. Souza, M. S. Strano, M. S. Dresselhaus, and M. A. Pimenta, *Phys. Rev. Lett.* **93**, 147406 (2004).
- ²² S. D. M. Brown, P. Corio, A. Marucci, M. S. Dresselhaus, M. A. Pimenta, and K. Kneipp, *Phys. Rev. B* **61**, R5137 (2000).
- ²³ A. Alexandrou, C. Trallero-Giner, G. L. Kanellis, and M. Cardona, *Phys. Rev. B* **40**, 1013 (1989).
- ²⁴ Y. Liu, R. Sooryakumar, E. S. Koteles, and B. Elman, *Phys. Rev. B* **45**, 6769 (1992).